

OPEN

Patient Dose Comparison for Intraoperative Imaging Devices Used in Orthopaedic Lumbar Spinal Surgery

Bria Moore, PhD
 K. Roland Womack, MS
 Giao Nguyen, MS
 Norah Foster, MD
 William Richardson, MD
 Terry Yoshizumi, PhD

From the Medical Physics Graduate Program, Duke University (Dr. Moore), Duke Radiation Dosimetry Laboratory, Duke University Medical Center (Dr. Moore, Mr. Womack, Ms. Nguyen, and Dr. Yoshizumi), the Department of Radiology, Duke University Medical Center (Dr. Yoshizumi), the Department of Medicine, Orthopedic Surgery, Duke University Medical Center, Durham, NC (Dr. Foster and Dr. Richardson), and U.S. Nuclear Regulatory Commission Region II, Atlanta, GA (Mr. Womack).

Correspondence to Dr. Yoshizumi: yoshi003@mc.duke.edu

Supported by U.S. Nuclear Regulatory Commission Health Physics Fellowship Grant No. NRC-HQ-12-G-38-0022 and Duke University Graduate Fellowship.

JAAOS Glob Res Rev 2018;2:e030

DOI: 10.5435/

JAAOSGlobal-D-18-00030

Copyright © 2018 The Authors. Published by Wolters Kluwer Health, Inc. on behalf of the American Academy of Orthopaedic Surgeons. This is an open-access article distributed under the terms of the Creative Commons Attribution-Non Commercial-No Derivatives License 4.0 (CCBY-NC-ND), where it is permissible to download and share the work provided it is properly cited. The work cannot be changed in any way or used commercially without permission from the journal.

Abstract

Background: The aim of this study was to determine the amount of radiation exposure from intraoperative imaging during two-level and four-level lumbar fusions.

Methods: Five imaging systems were studied: multidetector CT (MDCT) scanner (CT A); two mobile CT units (CT B and CT C); a C-arm (D); and fluoroscopy (E). Metal oxide semiconductor field effect transistor dosimeters measured doses at 25 organ locations using an anthropomorphic phantom. A fat-equivalent phantom was used to simulate an obese body mass index (BMI).

Results: The effective dose (ED) for C-arm D was estimated using commercial software. The ED for others was computed from the measured mean organ doses. EDs for a normal BMI patient, receiving a four-level fusion, are as follows: CT A (12.00 ± 0.30 mSv), CT B (5.90 ± 0.25 mSv), CT C (2.35 ± 0.44 mSv), C-arm D (0.44 mSv), and fluoroscopy E (0.30 ± 0.3 mSv). The rankings are consistent across all three BMI values except CT C and fluoroscopy E, which peaked in the overweight size because of system limitations. The other machines' ED trended with patient BMI.

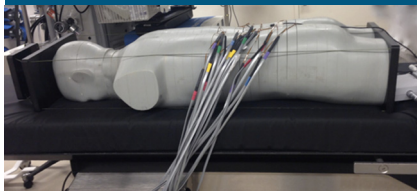
Conclusion: The dose reduction protocols were confirmed according to the manufacturer's specifications. The results of this study emphasize the need for the appropriate selection of the imaging system, especially because the type of device could have a substantial effect on patient radiation risk.

An increase in the American obesity rate has led to increased numbers of spinal complications requiring surgical intervention.^{1,2} The advancement of spinal surgery in recent years has led to an increased reliance on intraoperative imaging. With renewed demand, imaging technology has broadened to include a variety of different types, such as serial

radiography, C-arm fluoroscopy, and three-dimensional imaging. Typically, such technology is marketed directly to orthopaedic surgeons. In doing so, imaging protocols are often provided directly from the manufacturer. These settings are rarely optimized for specific-use cases such as spinal surgery.

Because most devices are calibrated to provide diagnostic-quality images,

Figure 1



Photograph showing the adult male anthropomorphic Model 701-D phantom (CIRS) with metal oxide semiconductor field effect transistors inserted for organ dosimetry.

the radiation dose is likely higher than that needed for surgical applications. Bone-soft tissue contrast is easy to achieve, and the spine is one of the largest organs in the body, so exceptional image quality is not needed. However, personnel radiation exposure has been shown to be increased in spinal surgery, specifically when compared with other orthopaedic specialties.³ For this reason, we can infer that the patient dose is also increased in this subspecialty of orthopaedics, although we are unaware of any published data on the patient dose in spinal surgery.

Our institution has the distinctive availability of several intraoperative imaging systems from which to select, including a multidetector CT (MDCT) scanner (CT A); two mobile CT units (CT B and CT C); a C-arm (D); and fluoroscopy (E). Although a number of studies have reported the radiation exposure of some of the modalities,^{4,5} and just recently, Hecht et al⁶ published the accuracy of instrumentation using CT B, we are unaware of any literature examining the radiation exposure of MDCT A or CT B. In addition, we are unaware of any study that has directly compared all

Table 1

Summary of Acquisition Parameters for MDCT A, CT B, and CT C

	Normal	Overweight	Obese
CT A			
Tube potential (kVp)	120	120	120
Beam current (mAs)	150	308	632
CT B			
Tube potential (kVp)	120	120	120
Beam current (mAs)	110	127.6	141
CT C			
Tube potential (kVp)	120	120	120
Beam current (mAs)	128	320	400

MDCT = multidimensional CT

these modalities with respect to commonly performed spinal surgery. This information is essential for any surgeon to accurately assess which intraoperative imaging modality best fits his or her risk-benefit profile.

Therefore, the aim of this study was to determine and compare the amount of radiation exposure to patients during two-level (three vertebral bodies) and four-level (five vertebral bodies) lumbar fusions using one of the five imaging systems available at a single institution.

Methods

CIRS Phantom

We used an adult male anthropomorphic phantom (Model 701-D; Computer Imaging Reference Systems [CIRS]) for patient radiation exposure. The phantom is designed to model a man weighing 72.6 kg (160 lbs) with a height of 1.73 m (5 feet 7 inches). The calculated body mass index of the phantom is 23.0,

which is considered within the normal range (18.5 to 24.9).⁷ Two layers of adipose-equivalent material were progressively added to increase the body mass index of the phantom to 28 (179 lbs) and 31 (198 lbs), placing the phantom within overweight and obese ranges, respectively. The phantom was placed prone on a carbon fiber table for all data acquisition. Figure 1 provides a representative image of the phantom position.

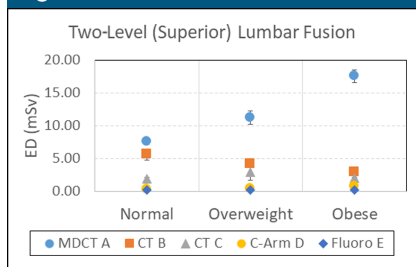
Metal Oxide Semiconductor Field Effect Transistor Calibration

High-sensitivity metal oxide semiconductor field effect transistor (MOSFET) detectors (Hi Sensitivity model 1002RD; Best Medical Canada) were calibrated in air, with each scanner in a stationary vertical-beam position based on previously established calibration methods.

C-arm D and fluoroscopy E automatically modulated tube potential and beam current based on patient thickness. By placing the phantom in

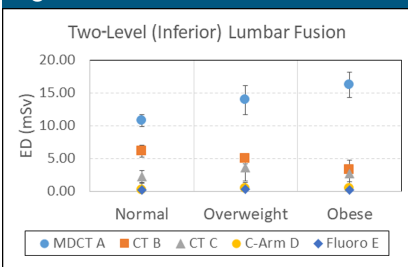
Dr. Richardson or an immediate family member is a member of a speakers' bureau or has made paid presentations on behalf of DePuy and Brainlab; serves as a paid consultant to DePuy, Spine Wave, Pfizer, and Trevana; has stock or stock options held in GYS-Tech; has received research or institutional support from NuVasive; and serves as a board member, owner, officer, or committee member of the American Academy of Orthopaedic Surgeons and North American Spine Society. None of the following authors or any immediate family member has received anything of value from or has stock or stock options held in a commercial company or institution related directly or indirectly to the subject of this article: Dr. Moore, Mr. Womack, Ms. Nguyen, Dr. Foster, and Dr. Yoshizumi.

Figure 2



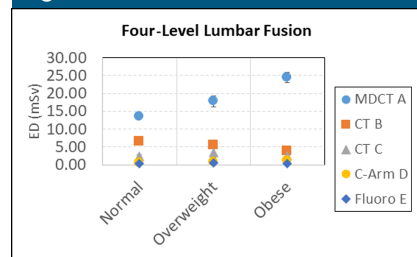
Graph showing the ED per scan for two-level lumbar fusions (superior fields of view). ED = effective dose

Figure 3



Graph showing the ED per scan for two-level lumbar fusions (inferior fields of view). ED = effective dose

Figure 4



Graph showing the ED per scan for four-level lumbar fusions. ED = effective dose

the beam, we determined an average tube potential to calibrate the MOSFET dosimeters.

CT Scan Parameters

Scan parameters were determined using patient protocols. MDCT A used beam current modulation based on an initial topogram image taken before each image series acquisition. CT B modulated the beam current based on input patient weight. Image acquisition parameters for MDCT A, CT B, and CT C are summarized in Table 1.

Fields of view (FOVs) were determined based on the procedure. In two-level fusions, two FOVs could be used: superior FOV, which captured lumbar vertebral levels 1 to 3 (L1-3), and the inferior FOV, which captured lumbar vertebral levels 3 to 5 (L3-5). Four-level fusions require visualizing all five lumbar vertebrae.

Organ Dosimetry

Skin entrance exposure was measured using a 0.18-mL ion chamber (Model 10X5-0.18; RadCal) with an electrometer (Model 9015; RadCal). Placement was adjusted per scan to ensure that the dosimeter was consistently within the FOV.

Twenty high-sensitivity dosimeters connected to four readers (Model TN-RD-16; Best Medical Canada) connected through a mobile MOSFET

wireless system (TN-RD-70-W20; Best Medical Canada) were used in data acquisition. MOSFET dosimeters were placed in 13 organ locations corresponding to the liver, spleen, active bone marrow in the thoracic spine, pancreas, kidneys, gall bladder, stomach, colon, active bone marrow in the lumbar spine, pelvis, and sacrum.

Effective Dose

The effective dose (ED) was calculated using the following equation:

$$ED \text{ (mSv)} = \sum PVCF_T * W_T * PD_T$$

where $PVCF_T$ represents the partial volume correction factor, W_T is the tissue weighting factor,⁸ and PD_T is the point dose for each organ, as determined experimentally. The partial volume correction factor was based on an estimation of the irradiated percentage of each organ volume.

All data were summarized using descriptive statistics. Data analysis was done using Microsoft Excel (versions 2010 and 2013; Microsoft).

Dose Reduction

The manufacturer of CT B offers a number of dose reduction modes, and we tested the dose reduction of three modes with a central ion chamber measuring the machine output. The

ion chamber measurement in the dose reduction modes was compared with the unadjusted dose output for an identical patient. We compared the measured exposure reduction with the manufacturer-quoted reduction.

Results

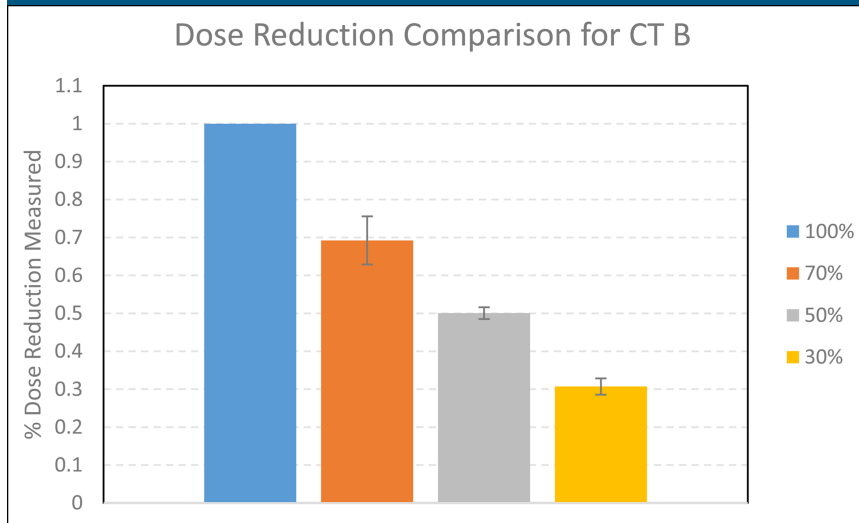
Effective Dose

Preliminary data showed that the dose output for fluoroscopy E was below the MOSFET measurement threshold. Because we were unable to acquire consistent point dose measurements, organ doses were acquired from the PCXMC (STUK), Monte Carlo-based patient dose modeling software, using measured beam quality factors.

The EDs are shown in Figures 2 through 4. All doses are reported per scan. In cases in which the machine was unable to cover all five lumbar vertebral bodies in a single FOV, five-level fusion data are reported as the dose sum of the superior and inferior FOV.

For the larger machines in which full coverage was feasible, three measurements—superior FOV, inferior FOV, and full FOV—were taken. Importantly, in this case, the inferior and superior views are not summed to calculate the full FOV dose. The full FOV dose was determined through a separate helical

Figure 5



Graph showing measured dose reduction for each manufacturer dose reduction setting.

scan that included all five vertebral levels, and because of overhanging effects, it may not be equivalent to the summed dose.

Dose Reduction

The manufacturer-stated reduction was found to be within $\pm 1\%$ of the measured reductions. Dose reduction data are shown in Figure 5.

Discussion

As expected, we found the dose to be on average $30\% \pm 3\%$ higher in four-level fusion studies than in two-level fusion studies across all patient sizes. We also noted a decrease in the percent difference between the superior and inferior FOV with increasing patient weight. This trend is likely due to the increased waist size created by the additional adipose layers. We also noted that the dose trends across patient weight were identical for all five machines in both two- and four-level fusions.

With increasing patient weight, we expect patient dose to increase as well, and in the case of MDCT A and C-arm

D, we found this to be true. However, CT B demonstrated a decrease in the patient dose with increasing patient weight. We attribute this finding to the fact that CT B was unable to adequately adjust output for above average-sized patients. CT C and fluoroscopy E showed a peak dose in overweight patients, indicating that the machine was appropriately adjusting to the increase in weight from normal to overweight, but that the machine was likely at maximum output for the obese patient.

In a normal patient with our largest FOV, the ED ranged from 0.34 to 13.52 mSv per scan. As the patient size increased, the dose range across the machines continued to widen. In addition, the dose from the single standard MDCT scanner investigated was substantially higher than that of any other machines. Across all three patients, the average difference was $154\% \pm 16\%$. In this case, because the dose is markedly higher, we can assume that the image quality metrics calibrated in this machine are likely well beyond what is needed in surgical applications; substantial dose reduction could be achieved

with optimized protocols. Our study did not investigate image quality.

The manufacturer's dose reduction settings appropriately adjusted CT B's output to reduce the dose. Although we did not repeat the internal organ measurements, we can infer from the reduction in the machine output that the EDs would adjust accordingly. The 50% dose reduction setting on CT B reduced normal patient dose from 6.16 mSv per scan to 2.91 mSv, an actual dose reduction of 53%. The reduction in obese and overweight patients is lower, 40% and 37%, respectively, but still a meaningful reduction, especially in cases requiring large numbers of scans. However, widespread implementation of these protocols would require a measure of image quality to ensure that the clinical outcomes are unaffected by the low-quality images.

A direct comparison of radiation exposure using our five intraoperative imaging systems has not been previously reported in the literature. We endeavored to compare the radiation exposure to patients during two-level and four-level lumbar fusions. By focusing on the ED measurement, we were able to combine the large number of organ doses we measured to use a single metric of comparison for all five machines. However, our ED calculation was limited by the fact that we did not measure the point dose in all organs. Previous studies verified our partial volume correction factor method with Monte Carlo modeling software.⁹

In addition, we acknowledge that our anthropomorphic phantom cannot truly model the heterogeneity of the human body or the breadth of variation in the patient cohort receiving spinal surgery. The addition of additional layers of soft tissue was an approximation of increasing obesity but certainly does not represent the heterogeneity of patient body habitus. We also acknowledge that our phantom could model only

patients up to the borderline classification of obesity; in markedly overweight patients, the dose trends may not hold. Our phantom model is sufficient in this use case, that is, dose output comparisons.

Conclusion

Our work has demonstrated a wide range of patient doses from different imaging systems used for an identical purpose. This observation is highly concerning because the patient outcome should be independent of equipment choice. This study provides surgeons with radiation exposure comparison data for five different imaging systems in order to help them make educated decisions regarding the risks and benefits of utilization. Additional studies on spinal imaging modalities are needed, and future endeavors may include comparative analyses of image qual-

ity or experimenting with lower radiation dose settings available with some systems. Importantly, continued efforts are also needed to inform other surgical teams to use the physics support in their institution when purchasing imaging systems.

References

1. Shiri R, Karppinen J, Leino-Arjas P, Solovieva S, Viikari-Juntura E: The association between obesity and low back pain: A meta-analysis. *Am J Epidemiol* 2010; 171:135–154.
2. Liuke M, Solovieva S, Lamminen A, et al: Disc degeneration of the lumbar spine in relation to overweight. *Int J Obes (Lond)* 2005;29:903–908.
3. Nelson EM, Monazzam SM, Kim KD, Seibert JA, Klineberg EO: Intraoperative fluoroscopy, portable x-ray, and CT: Patient and operating room personnel radiation exposure in spinal surgery. *Spine J* 2014;14: 2985–2991.
4. Tabaraee E, Gibson AG, Karahalios DG, Potts EA, Mobasser JP, Burch S: Intraoperative cone beam-computed tomography with navigation (O-ARM) versus conventional fluoroscopy (C-ARM): A cadaveric study comparing accuracy, efficiency, and safety for spinal instrumentation. *Spine (Phila Pa 1976)* 2013;38:1953–1958.
5. Stuby F, Seethaler AC, Shiozawa T, et al: Evaluation of image quality of two different three-dimensional cone-beam-scanners used for orthopedic surgery in the bony structures of the pelvis in comparison with standard CT scans [German]. *Z Orthop Unfall* 2011;149: 659–667.
6. Hecht N, Kamphuis M, Czabanka M, et al: Accuracy and workflow of navigated spinal instrumentation with the mobile AIRO® CT scanner. *Eur Spine J* 2016;25: 716–723.
7. Centers for Disease Control and Prevention: *Healthy Weight—It's Not a Diet, It's a Lifestyle!* 2015. http://www.cdc.gov/healthyweight/assessing/bmi/adult_bmi/index.html. Accessed December 6, 2017.
8. The 2007 Recommendations of the International Commission on Radiological Protection: ICRP Publication 103. *Ann ICRP* 2007;37:1–332.
9. Januzis N, Nguyen G, Frush DP, Hoang JK, Lowry C, Yoshizumi TT: Feasibility of using the computed tomography dose indices to estimate radiation dose to partially and fully irradiated brains in pediatric neuroradiology examinations. *Phys Med Biol* 2015;60: 5699–5710.